LETTERS
PUBLISHED ONLINE: 1 AUGUST 2010 | DOI: 10.1038/NPHYS1735
nature physics

Quasiparticle lifetimes in metallic quantum-well nanostructures

Patrick S. Kirchmann[1,2], Laurenz Rettig[1], Xabier Zubizarreta[3,4], Vyacheslav M. Silkin[3,4,5], Evgueni V. Chulkov[3,4,6] and Uwe Bovensiepen[1,7]*

Quasiparticle lifetimes in metals as described by Fermi-liquid theory[1] are essential in surface chemistry[2] and determine the mean free path of hot carriers[3]. Relaxation of hot electrons is governed by inelastic electron–electron scattering, which occurs on femtosecond timescales owing to the large scattering phase space competing with screening effects[4]. Such lifetimes are widely studied by time-resolved two-photon photoemission[5,6], which led to understanding of electronic decay at surfaces[6–8]. In contrast, quasiparticle lifetimes of metal bulk[5,9–12] and films[11,13–15] are not well understood because electronic transport[10,16,17] leads to experimental lifetimes shorter than expected theoretically[13,15,18]. Here, we lift this discrepancy by investigating Pb quantum-well structures on Si(111), a two-dimensional model system[19–29]. For electronic states confined to the film by the Si bandgap we find quantitative agreement with Fermi-liquid theory and *ab initio* calculations[4,7] for bulk Pb, which we attribute to efficient screening. For states resonant with Si bands, extra decay channels open for electron transfer to Si, resulting in lifetimes shorter than expected for bulk. Thereby we demonstrate that for understanding electronic decay in nanostructures coupling to the environment is essential, and that even for electron confinement to a few ångströms Fermi-liquid theory for bulk can remain valid.

We begin the discussion by analysing the quantized electronic structure in epitaxially grown Pb films. Figure 1a shows the photoemission intensity in a colour map as a function of Pb film thickness. We probe occupied states at energies below the Fermi level E_F by one-photon photoemission (1PPE) with a photon energy $h\nu$ larger than the work function $E_F - E_{vac}$ and unoccupied states above E_F by two-photon photoemission (2PPE), where the sum of both photon energies $h\nu_1 + h\nu_2$ is larger than the work function. These linear and nonlinear methods of photoemission are illustrated in Fig. 1, left. Symbols denote the peak positions of Lorentzian line fits. In Fig. 1b the fitting results are shown for three exemplary Pb thicknesses; details are given in the Supplementary Information. The data exhibit three branches of occupied quantum-well states (QWSs) and five branches of unoccupied QWSs that disperse towards E_F with increasing coverage. The binding energies $(E - E_F)$ of the lowest unoccupied QWS (luQWS) oscillate between 1.65 and 0.6 eV by 45–165% on variation by one monolayer (1 ML) in thickness from N to $N+1$ ML and form the two lowest branches of unoccupied QWSs. Simultaneously, the QWS peaks exhibit a high intensity contrast owing to an efficient electron confinement to the film at energies of the Si bandgap. Hence, the study of electron dynamics of the luQWS is especially interesting because this state resides in the Si bandgap for even N and is confined to the film. In contrast, for odd N the luQWS is degenerate with Si bands. The thickness-dependent 1PPE results probe the quantized occupied electronic states[21,23], confirm our earlier laser photoemission observations[24] and are used as a thickness reference.

Delaying the two laser pulses at energies $h\nu_1$ and $h\nu_2$ employed in 2PPE with respect to each other enables us to study the decay of hot quasiparticles directly in the time domain in a pump–probe experiment. Figure 2 shows the electron population decay in the time domain by cross-correlation traces of the luQWS as a function of N. For odd N a fast population decay is observed, which slows down with increasing thickness. In contrast, for even N a slower and thickness-independent decay is found. The quasiparticle lifetimes are evaluated from a fit of a rate-equation model that is convoluted with the laser-pulse envelope[30]. This model enables us to determine the hot-electron lifetimes independently from a delayed population build-up due to secondary electrons; see also Supplementary Information. Essentially, the lifetimes are given by the inverse slope of the initial population decay, $\tau = \hbar/\Gamma$, as indicated in Fig. 2. At later delays (odd N: >150–200 fs/even N: >800 fs) a second slower decay component is observed, which, however, does not contribute significantly to the initial decay dynamics at earlier delays[30].

Figure 3 summarizes the coverage-dependent quasiparticle lifetimes τ in Pb/Si(111). As evident from Fig. 2, τ oscillates with a 2 ML period, which is correlated to the characteristic binding-energy variation[19]; see Fig. 1. For odd N, the lifetimes depend on the coverage and increase from $\tau = 5(5)$ fs for 1 ML to 37(5) fs for 15 ML. This is in contrast to even N, where the lifetimes are constant at $\tau = 115(10)$ fs within the experimental accuracy. Hence, the lifetimes change by 200–2,000% when the film thickness is changed by 1 ML from odd to even N. On the one hand, the lifetimes seem to be correlated to the energetic position of the respective luQWS with respect to the Si bandgap: when the luQWS is degenerate with the Si bands we might expect a faster decay owing to extra decay and transport channels that open up towards the substrate. On the other hand, the binding energy of the luQWS oscillates with the characteristic 2 ML period (Fig. 1). In turn, the oscillating binding energies of the luQWS alone can introduce periodic changes of the phase space for electron–electron (e–e) scattering processes and thereby can lead to the observed lifetime oscillations.

[1]Fachbereich Physik, Freie Universität Berlin, Arnimallee 14, D-14195 Berlin-Dahlem, Germany, [2]Stanford Institute for Material and Energy Science, 476 Lomita Mall, Stanford, 94305, California, USA, [3]Donostia International Physics Center (DIPC), Paseo de Manuel Lardizabal, 4, 20018 San Sebastian/Donostia, Basque Country, Spain, [4]Departamento de Física de Materiales, Facultad de Ciencias Químicas, UPV/EHU, Apdo. 1072, 20080 San Sebastián, Basque Country, Spain, [5]IKERBASQUE, Basque Foundation for Science, 48011 Bilbao, Basque Country, Spain, [6]Centro de Física de Materiales CFM - Materials Physics Center MPC, Centro Mixto CSIC-UPV/EHU, Edificio Korta, Avenida de Tolosa 72, 20018 San Sebastián, Spain, [7]Fakultät für Physik, Universität Duisburg-Essen, Lotharstr. 1, D-47048 Duisburg, Germany. *e-mail: uwe.bovensiepen@uni-due.de.

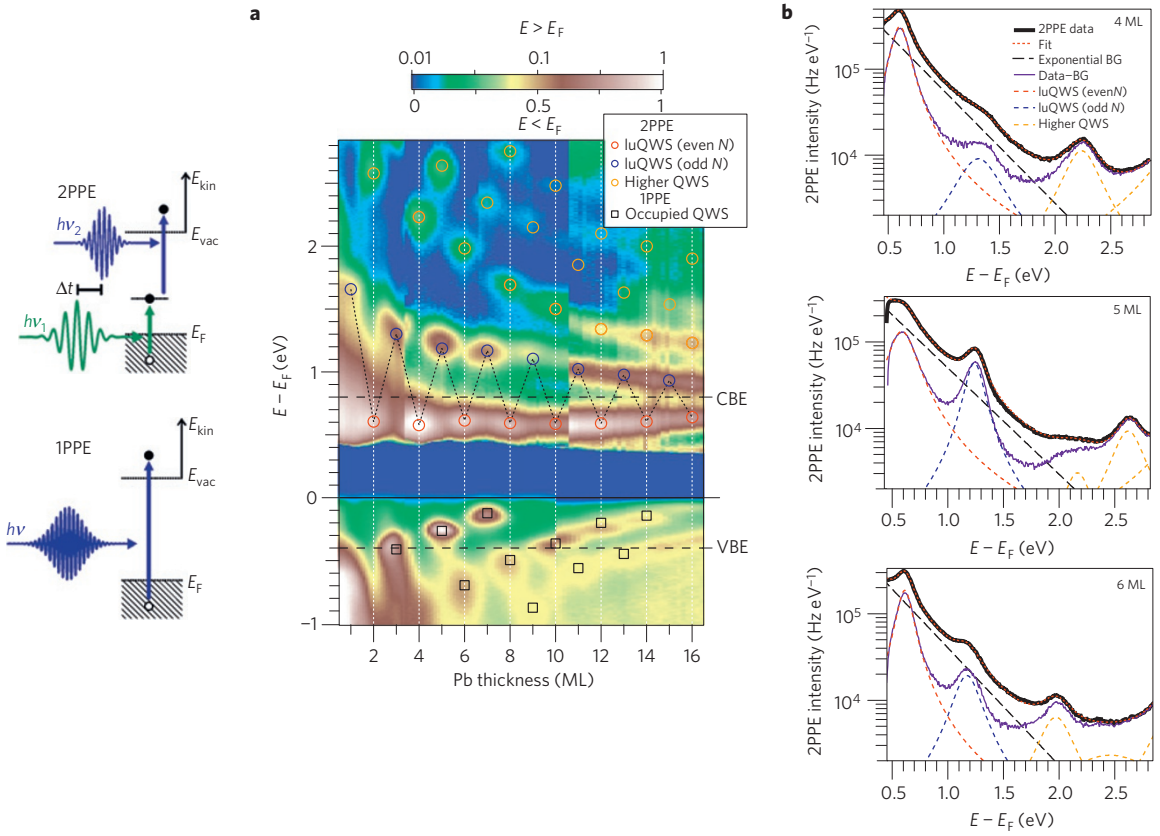

Figure 1 | Quantized band structure of Pb/Si(111) for the occupied and unoccupied density of states at the $\bar{\Gamma}$ point observed by photoemission. **a**, Photoemission intensity in a colour map as a function of Pb thickness N in ML for the occupied and unoccupied states analysed by 1PPE and 2PPE, respectively. The 2PPE intensity is shown on a logarithmic scale, whereas the 1PPE intensity is plotted on a linear scale. The requirement that the sample work function is smaller than $h\nu$ in 2PPE prevented us from accessing energies $E - E_F < 300$ meV in these particular experiments. Red (blue) circles indicate the binding energies of the luQWS for even (odd) N; yellow circles indicate higher-lying QWSs. The binding energies are determined from a Lorentzian line fit as explained in **b** and the Supplementary Information. The horizontal dashed lines indicate the positions of the valence- and conduction-band edges (VBE/CBE). The 2 ML oscillation period of the binding energy of the luQWS is emphasized by a dotted line. The image is composed from three overlapping data sets; in total, 109 spectra have been analysed for this figure. **b**, 2PPE spectra for three exemplary values of N. The data are fitted by Lorentzian peaks and an exponentially decaying background (BG) and convoluted with a Gaussian instrument function. Background subtraction enhances the contrast between QWSs for odd and even N; see Supplementary Information.

To distinguish these two limiting cases the quasiparticle lifetimes are plotted versus the binding energy $E - E_F$ of the luQWS in Fig. 4a. Fermi-liquid theory (FLT) for bulk materials with three-dimensional bands predicts a quadratic scaling law of the inelastic e–e scattering rate $\Gamma_{e-e} = \hbar/\tau_{e-e}$ of the excited quasiparticle with respect to the excess energy above the Fermi level $\xi = E - E_F$

$$\Gamma_{e-e} = \frac{\hbar}{\tau_{e-e}} = \frac{e_0 {m_e}^{3/2}}{32\, 3^{5/6} \pi^{2/3} \epsilon_0^{1/2} \hbar^3} n^{-5/6} \xi^2 = \alpha \xi^2$$

Here, n, e_0, m_e and ϵ_0 denote the bulk electron density, the elementary charge, the free-electron mass and the vacuum permittivity, respectively.

Clearly, the measured data points are reproduced on an absolute scale using FLT (ref. 1) and employing the electron density of bulk Pb, $n_{Pb} = 13.2 \times 10^{28}$ m^{-3}. As n is given only by the size of the unit cell and the number of valence electrons, the FLT curve may be regarded as a parameter-free description. It is surprising that, despite the two-dimensional character of the film band structure[20–22,24,25,27], the lifetimes scale quadratically with the excess energy ξ and hence exhibit a clear FLT behaviour. This can be justified by the strong screening of the Coulomb interaction in Pb films. If the screening length λ_s were larger than the typical thickness of the metal film we could expect finite-size effects reflected in the intensity of the e–e scattering. In this two-dimensional limit the screening would be reduced and could promote more intense e–e scattering, leading to shorter lifetimes than in the bulk[1]. To compare the electronic screening in the metal film with the typical layer thickness, the three-dimensional Thomas–Fermi screening length[1] in Pb

$$\lambda_s = \frac{1}{2}\sqrt{a_0 \left(\frac{\pi}{3n}\right)^{1/3}} = 0.51\,\text{Å}$$

where a_0 denotes the Bohr radius, is compared with the interlayer spacing of $d_{[111]} = 2.86$ Å normal to the film. As $\lambda_s < d_{[111]}$ even a free-standing Pb(111) film of 1 ML thickness should exhibit three-dimensional screening. In addition, the energy-dependent quasiparticle lifetime in bulk Pb from an *ab initio* calculation employing the *GW* approximation[4,7] is shown in Fig. 4a and is very similar to the FLT dependence. Owing to the agreement of the experimental and theoretical results, we conclude that the quasiparticle lifetimes are (1) dominated by e–e scattering that (2) follows the expectation from simple FLT for bulk materials.

This behaviour is consistent with the response function we have calculated for bulk Pb, which does not show any sharp feature

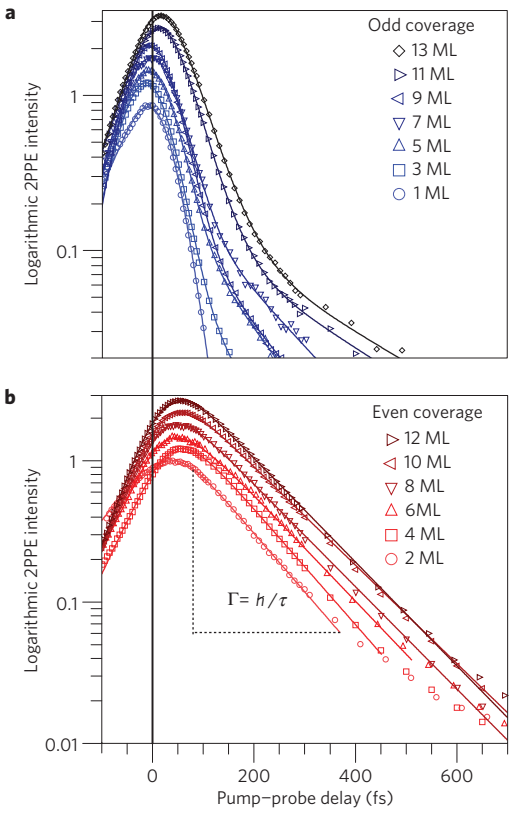

Figure 2 | Decay of the transient quasiparticle population in the luQWS for various *N*. a,b, Cross-correlation traces for odd and even *N*, respectively, on a logarithmic intensity scale. Symbols indicate the 2PPE intensity obtained at $h\nu_1 = 1.88$ eV and $h\nu_2 = 3.77$ eV pump and probe photon energy by integrating the transient 2PPE intensity over an energy window of 100 meV width. The fast initial population decay time for odd *N* decreases with coverage, whereas the decay time for even *N* is slower and coverage independent. Solid lines are fits of a rate-equation model[30] (see also the Supplementary Information), which yields the decay times that are discussed in Figs 3 and 4.

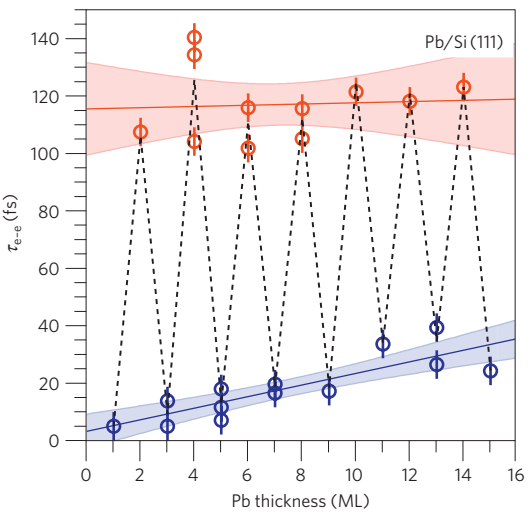

Figure 3 | Lifetime of the luQWS as a function of Pb thickness. The solid lines are linear fits to guide the eye; the shaded areas indicate a 90% confidence interval of the fits. The error bars of the analysed electron lifetimes amount to ±5 fs and are determined by the statistical error of the data and the fitting procedure.

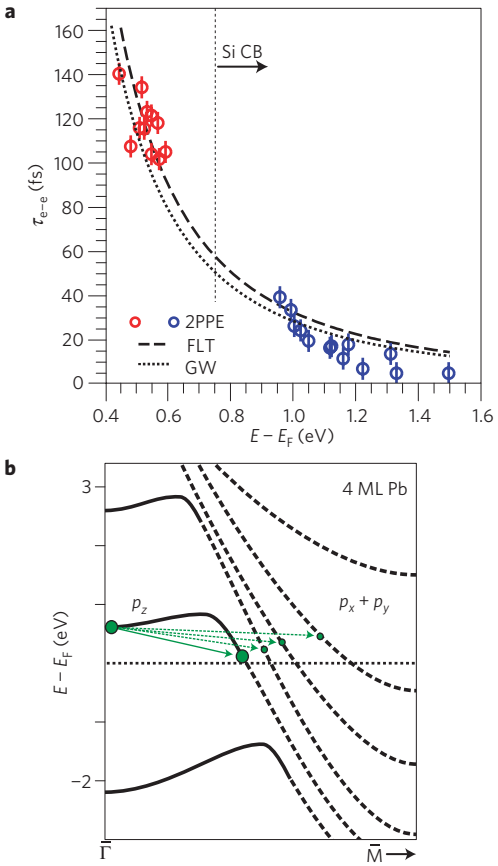

Figure 4 | Comparison of the measured quasiparticle lifetimes with theoretical results from FLT and the *GW* approximation. a, Analysis of the quasiparticle lifetimes of the luQWS as a function of binding energy. The error bars of the analysed electron lifetimes amount to ±5 fs and are determined by the statistical error of the data and the fitting procedure. The dashed and dotted lines indicate the expectation from FLT (ref. 1) and the *GW* approximation[4,7] for bulk Pb, respectively. The Si CBE is indicated. **b**, Scheme of the quantized band structure of a 4 ML freestanding Pb film. The solid lines indicate weakly dispersing bands near $\bar{\Gamma}$ with mostly p_z symmetry, whereas the dashed lines indicate strongly dispersing bands near $\bar{M}$ with partial p_x and p_y orbital character. The dashed arrows depict interband scattering of hot electrons into bands with partial p_x and p_y character. The solid arrow represents intraband scattering within the same band of p_z symmetry.

in the energy interval of interest up to $\xi = 1.6$ eV. Additionally, the binding energies of the luQWS in the Pb film are small compared with the energy of $E_F \approx 10$ eV with respect to the band bottom. In this situation the imaginary part of the screened Coulomb interaction, being a linear function of energy, can be decomposed into a product of one energy-dependent and one energy-independent function[7]. Within the *GW* approximation[7] this results directly in the quadratic dependence of Γ_{e-e} on ξ.

The Fermi-liquid character of Pb films accounts for a constant lifetime for the luQWS with even *N* (Fig. 3) because the binding energy of the state does not vary with thickness (Fig. 1). Further conclusions with respect to this constant lifetime can be drawn from the symmetry of the states contributing to the decay, as shown in Fig. 4b. In the vicinity of $\bar{\Gamma}$ the QWSs are weakly dispersing (solid lines) and of p_z symmetry. Towards $\bar{M}$ they acquire p_x, p_y character (dashed lines) and disperse more strongly. This leads to two different decay channels at $\bar{\Gamma}$: (1) intraband scattering with a final state of dominant p_z character (solid arrow) and (2) interband scattering into final states with partial p_x and p_y character (dashed

arrows). The latter would lead to thickness-dependent decay rates as the respective final-state density in the interband process changes as a function of N. However, this process might have a low scattering rate owing to the different orbital character of initial and final states leading to a small scattering cross-section[7]. From the observed absence of a thickness dependence in the lifetime for even N within the investigated range from 1 to 15 ML (see Methods), we conclude that intraband scattering dominates.

Having explained the lifetimes of even N, we address the increasing lifetime with thickness for odd N. This behaviour can also be understood by FLT, because with increasing thickness the binding energy shifts towards E_F, leading to a decreasing phase space for e–e scattering. A closer inspection reveals a systematic deviation from FLT at $\xi > 1.2$ eV. We attribute this to an extra decay channel, namely electron transfer into the substrate, because at these energies the states are degenerate with the Si conduction band.

Methods

The experimental set-up and procedures have been described in detail elsewhere[17,24]. In brief, wedges[31,32] of epitaxial Pb films are grown on the Si(111)-$\sqrt{3}\times\sqrt{3}$-R30°-Pb reconstruction by evaporation of Pb under ultrahigh-vacuum conditions[23,24] (base pressure $< 1\times10^{-10}$ mbar). During preparation the temperature was kept at 100 K to avoid island formation and surface diffusion. The evaporation rate of 0.5–1 ML min^{-1} was monitored by a quartz crystal microbalance and cross-checked after deposition by comparison of the observed binding energies of occupied QWSs (ref. 24) with density functional calculations[19]. Furthermore, the discrete QWSs only appear at integer Pb thicknesses, providing an intrinsic coverage calibration. For characterization of the unoccupied electronic structure and the analysis of the electron dynamics, Pb wedges are grown with a thickness gradient of 1–2 ML mm^{-1}. Together with the laser spot size of ∼100 μm, this corresponds to a coverage resolution of 0.1–0.2 ML.

For the 2PPE experiments, which address the unoccupied part of the band structure, the output of an amplified Ti:sapphire laser system (Coherent RegA 9050) operating at 300 kHz repetition rate is used to drive a tunable optical parametric amplifier. The signal at $h\nu_1 = 2.7$–1.7 eV is frequency doubled in a β-barium borate crystal into the ultraviolet wavelength range, $h\nu_2 = 5.4$–3.4 eV. These time-correlated pairs of femtosecond pump and probe laser pulses, $h\nu_1$ and $h\nu_2$, respectively, are focused into the ultrahigh-vacuum chamber and spatially overlapped on the sample surface with typical focus diameters of 100 μm. Typical pump fluences are of the order of 50–100 μJ cm^{-2} and the overall time resolution is 60 fs. Alternatively, the RegA output is frequency quadrupled to yield $h\nu = 6.2$ eV for the characterization of the occupied electronic structure with 1PPE.

The binding energy of the photoemitted electrons is determined from their kinetic energy E_{kin} analysed in a time-of-flight spectrometer: $E - E_F = E_{kin} + \Phi - h\nu$. Here, Φ denotes the spectrometer work function and $h\nu$ the photon energy of the probing laser pulse. All measurements were made at a sample temperature of 100 K and in normal emission geometry at the $\overline{\Gamma}$ point.

The relativistic *ab initio* calculations of the quasiparticle lifetimes were carried out in the framework of the *GW* approximation[4,7]. The energy-dependent quasiparticle lifetimes $\tau_{e-e}(E) = 1/\Gamma_{e-e}(E)$ are estimated for the $6p_z$ parent bulk band dispersing along Γ–L.

Received 9 September 2009; accepted 24 June 2010; published online 1 August 2010

References

1. Giuliani, G. F. & Vignale, G. *Quantum Theory of the Electron Liquid* (Cambridge Univ. Press, 2005).
2. Zhu, X-Y. Electronic structure and electron dynamics at molecule–metal interfaces: Implications for molecule-based electronics. *Surf. Sci. Rep.* **56,** 1–83 (2004).
3. Kliewer, J. *et al.* Dimensionality effects in the lifetime of surface states. *Science* **288,** 1399–1402 (2000).
4. Chulkov, E. V. *et al.* Electronic excitations in metals and at metal surfaces. *Chem. Rev.* **106,** 4160–4206 (2006).
5. Petek, H. & Ogawa, S. Femtosecond time-resolved two-photon photoemission studies of electron dynamics in metals. *Prog. Surf. Sci.* **56,** 239–310 (1997).
6. Weinelt, M. Time-resolved two-photon photoemission from metal surfaces. *J. Phys. Condens. Mater.* **14,** R1099–R1141 (2002).
7. Echenique, P. M. *et al.* Decay of electronic excitations at metal surfaces. *Surf. Sci. Rep.* **52,** 219–317 (2004).
8. Güdde, J., Rohleder, M., Meier, T., Koch, S. W. & Höfer, U. Time-resolved investigation of coherently controlled electric currents at a metal surface. *Science* **318,** 1287–1291 (2007).
9. Schmuttenmaer, C. A. *et al.* Time-resolved two-photon photoemission from Cu(100): Energy dependence of electron relaxation. *Phys. Rev. B* **50,** 8957–8960 (1994).
10. Knoesel, E., Hotzel, A. & Wolf, M. Ultrafast dynamics of hot electrons and holes in copper: Excitation, energy relaxation, and transport effects. *Phys. Rev. B* **57,** 12812–12824 (1998).
11. Cao, J., Gao, Y., Elsayed-Ali, H. E., Miller, R. J. D. & Mantell, D. A. Femtosecond photoemission study of ultrafast electron dynamics in single-crystal Au(111) films. *Phys. Rev. B* **58,** 10948–10952 (1998).
12. Gerlach, A. *et al.* Lifetime of *d* holes at Cu surfaces: Theory and experiment. *Phys. Rev. B* **64,** 085423 (2001).
13. Ogawa, S., Nagano, H. & Petek, H. Optical intersubband transitions and femtosecond dynamics in Ag/Fe(100) quantum wells. *Phys. Rev. Lett.* **88,** 116801 (2002).
14. Wegner, D., Bauer, A. & Kaindl, G. Electronic structure and dynamics of quantum-well states in thin Yb metal films. *Phys. Rev. Lett.* **94,** 126804 (2005).
15. Zhukov, V. P. *et al.* Excited electron dynamics in bulk ytterbium: Time-resolved two-photon photoemission and GW + T *ab initio* calulations. *Phys. Rev. B* **76,** 193107 (2007).
16. Aeschlimann, M. *et al.* Transport and dynamics of optically excited electrons in metals. *Appl. Phys. A* **71,** 485–491 (2000).
17. Lisowski, M., Loukakos, P. A., Bovensiepen, U. & Wolf, M. Femtosecond dynamics and transport of optically excited electrons in epitaxial Cu films on Si(111)-7 × 7. *Appl. Phys. A* **79,** 739–741 (2004).
18. Bauer, M., Pawlik, S. & Aeschlimann, M. Electron dynamics of aluminum investigated by means of time-resolved photoemission. *Proc. SPIE* **3272,** 201–210 (1998).
19. Wei, C. M. & Chou, M. Y. Theory of quantum size effects in thin Pb(111) films. *Phys. Rev. B* **66,** 233408 (2002).
20. Guo, Y. *et al.* Superconductivity modulated by quantum size effects. *Science* **306,** 1915–1917 (2004).
21. Upton, M. H., Wei, C. M., Chou, M. Y., Miller, T. & Chiang, T-C. Thermal stability and electronic structure of atomically uniform Pb films on Si(111). *Phys. Rev. Lett.* **93,** 026802 (2004).
22. Zhang, Y-F. *et al.* Band structure and oscillatory electron–phonon coupling of Pb thin films determined by atomic-layer-resolved quantum-well states. *Phys. Rev. Lett.* **95,** 096802 (2005).
23. Dil, J. H., Kim, J. W., Kampen, T., Horn, K. & Ettema, A. R. H. F. Electron localization in metallic quantum wells: Pb versus In on Si(111). *Phys. Rev. B* **73,** 161308 (2006).
24. Kirchmann, P. S., Wolf, M., Dil, J. H., Horn, K. & Bovensiepen, U. Quantum size effects in Pb/Si(111) investigated by laser-induced photoemission. *Phys. Rev. B* **76,** 075406 (2007).
25. Shanenko, A. A., Croitoru, M. D. & Peeters, F. M. Oscillations of the superconducting temperature induced by quantum well states in thin metallic films: Numerical solution of the Bogoliubov–de Gennes equations. *Phys. Rev. B* **75,** 014519 (2007).
26. Hong, I-P. *et al.* Decay mechanisms of excited electrons in quantum-well states of ultrathin Pb islands grown on Si(111): Scanning tunneling spectroscopy and theory. *Phys. Rev. B* **80,** 081409 (2009).
27. Qin, S., Kim, J., Niu, Q. & Shih, C-K. Superconductivity at the two-dimensional limit. *Science* **324,** 1314–1317 (2009).
28. Brun, C. *et al.* Reduction of the superconducting gap of ultrathin Pb islands grown on Si(111). *Phys. Rev. Lett.* **102,** 207002 (2009).
29. Zhang, T. *et al.* Superconductivity in one-atomic-layer metal films grown on Si(111). *Nature Phys.* **6,** 104–108 (2010).
30. Kirchmann, P. S. & Bovensiepen, U. Ultrafast electron dynamics in Pb/Si(111) investigated by two-photon photoemission. *Phys. Rev. B* **78,** 035437 (2008).
31. Kawakami, R. K. *et al.* Quantum-well states in copper thin films. *Nature* **398,** 132–134 (1999).
32. Paggel, J. J., Miller, T. & Chiang, T-C. Quantum-well states as Fabry–Pérot modes in a thin-film electron interferometer. *Science* **283,** 1709–1711 (1999).

Acknowledgements

We thank C. Brun for discussions and acknowledge support from and discussions with M. Wolf. This work has been funded by the Deutsche Forschungsgemeinschaft through BO 1823/2 and by the Ministerio de Ciencia y Tecnologia (grant FIS2007-66711-C02-01). P.S.K. acknowledges support by the International Max-Planck Research School 'Complex Surfaces in Material Science'.

Author contributions

P.S.K. and L.R. carried out the experiments and analysed the data; U.B. designed and coordinated the experiment; X.Z. and V.M.S. carried out the calculations; P.S.K., U.B., and E.V.C. wrote the paper; all authors commented on the manuscript.

Additional information

The authors declare no competing financial interests. Supplementary information accompanies this paper on www.nature.com/naturephysics. Reprints and permissions information is available online at http://npg.nature.com/reprintsandpermissions. Correspondence and requests for materials should be addressed to U.B.